# Sensing of Vaporous Organic Compounds by $TiO_2$ Porous Films Covered with Polythiophene Layers

*Mutsumi Kimura,* Ryousuke Sakai, Seiko Sato, Tadashi Fukawa, Tsuyoshi Ikehara, Ryutaro Maeda, and Takashi Mihara*

**This paper describes the detection of volatile organic compounds (VOCs) through analyses of two output signals from integrated microcantilever sensor arrays coated with organic-inorganic hybrid sensing layers. The surface of $TiO_2$ porous films was modified by amphiphilic terthiophene monomers and the adsorbed monomers were polymerized at the surface of $TiO_2$ nanoparticles. The $TiO_2$ porous films covered with polythiophene layers worked as highly sensitive sensing interfaces to provide two output signals for weight and resistance changes during exposure to VOC vapor. When the $TiO_2$ porous films onto the sensor arrays were dyed with various kinds of amphiphilic monomers with different substituents, the resulting films provide exact information on VOC concentration from the mass changes as well as VOC classification from the analyses of response patterns.**

## 1. Introduction

We are constantly exposed to health and safety hazards as a result of dynamic and unpredictable conditions. On-site and real-time analyses of ambient information on factors such as sounds, colors, and odors provide us with situational awareness to manage these hazards. Among the ambient factors, odorants are detected and discriminated though olfaction and the physicochemical properties of odorants to induce specific odor sensations by selective binding with odorant receptors in the nasal cavity. The chemical features of the odorants activate multiple receptors and all of the signals are sent to the brain as activation patterns to recognize a specific group or feature of the target odorant.[1]

Artificial electronic-nose systems have been developed for the detection of volatile odorants. These systems mimic the mammalian olfactory system by producing sensing patterns of cross-responsive sensor arrays.[2,3] The systems comprise a chemical sensor array together with an interfacing electronic circuitry as well as a pattern-recognition unit that acts as a signal-processing system. The chemical sensor arrays are capable of converting chemical information into an output signal and each sensor in the array can generate different signals in response to the concentration and the specific interaction with target odorants. Target odorants cannot be identified from the response of a single sensor element.[4–6] A response pattern from multiple sensors in the arrays can provide a fingerprint that allows classification and identification of the odorant. To achieve a sensing patterns, a variety of sensing layers with different responses for odorants is required.

Mass sensors have been applied to chemical sensing in the electronic-nose systems by the use of various sensing materials.[2,3] When volatile organic compounds (VOCs) are captured within the sensing layers on the mass sensors, the sorption amounts can be monitored by resonant frequency shifts of the sensors. The determination of weight changes is directly related to the interactions between the sensing layers and target compounds. Quartz crystal microbalances (QCMs) have been widely used as the platform for mass sensing by the deposition with the sensing layers.[7] Their resonance frequency has been proven to decrease linearly upon the increase of weight on the QCM electrode in a nanogram level. Recently, silicon resonators such as microcantilevers and microdisks are expected to provide an alternative platform for mass sensors.[8] The microfabrication processes of silicon makes it possible to significantly downsize of sensor arrays and integrate various components onto one chip.

For all chemical-sensor technology, the sensor surface promotes the interaction between the sensor and the target compounds that produces the sensor responses. To date, semiconductor nanoparticles with a narrow diameter distribution have been prepared from oxides and chalcogenides of various metals and these nanoparticles have been packed to form porous films.[9] These porous films increase the active surface by several orders of magnitude and have many enhanced properties. Moreover, the surface of semiconductor nanoparticles can be modified with a monolayer of adsorbed organic molecules. Highly efficient dye-sensitized solar cells have been developed by attaching dye molecules to nanocrystalline films of anatase

Prof. M. Kimura, R. Sakai, S. Sato, T. Fukawa
Department of Functional Polymer Science
Faculty of Textile Science and Technology
Shinshu University
Ueda 386-8567, Japan
E-mail: mkimura@shinshu-u.ac.jp
Dr. T. Ikehara, Dr. R. Maeda
National Institute of Advanced Industrial Science and Technology (AIST)
1-2 Namiki, Tsukuba 305-8564, Japan
Dr. T. Mihara
Future Creation Laboratory
Olympus Corporation, Tokyo 192-8512, Japan

**DOI: 10.1002/adfm.201101953**

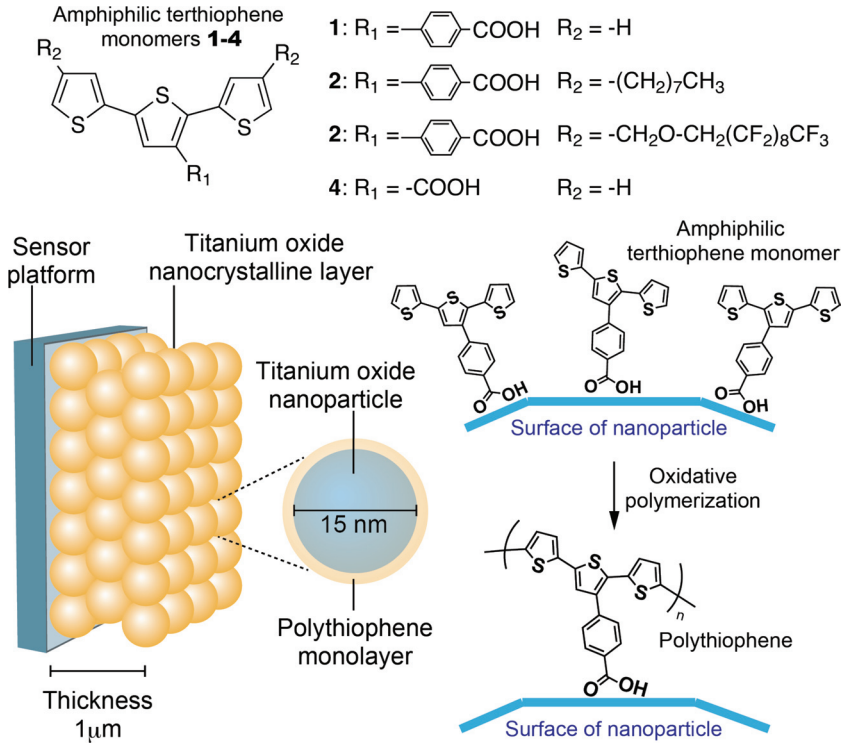


**Figure 1.** Modification of $TiO_2$ surface with amphiphilic terthiophene monomers **1** – **4**.

titanium oxide ($TiO_2$).[10] A large surface area of porous $TiO_2$ films is a most important key for enhancing the light-to-electricity conversion yield of the photovoltaic systems. We synthesized a novel series of amphiphilic terthiophene monomers with one carboxylic acid. The synthesized terthiophene derivatives were adsorbed onto the surface of nanocrystalline $TiO_2$ particles and the adsorbed terthiophenes were polymerized by electrochemical or chemical oxidation (**Figure 1**). The covering of $TiO_2$ particles with a polythiophene monolayer affected the responsibility and selectivity of VOC sensing. Although films of conjugated polymers and metal oxides have been used as sensing layers in electronic noses.[11–19] There have no previous reports of organic–inorganic hybrid porous films composed of metal oxide nanoparticles covered with conjugated polymer monolayers for use as the sensing layer for VOC sensing. Here, we report the detection of VOCs by a mictrocantilever sensor array using porous $TiO_2$ films covered with polythiophene monolayers.

## 2. Results and Discussion

Packing nanocrystalline $TiO_2$ particles with a uniform diameter can form a porous structure with a large active surface area. When a 20 μg $TiO_2$ porous film (120 $m^2$ $g^{-1}$ specific surface area) was deposited on the surface of QCMs (0.19 $cm^2$ gold electrode area), the porous films have roughly 20 times the surface area compared to nonporous films. Porous structures promote a rapid penetration of gaseous molecules and provide an obvious advantage in improving the response of VOC sensing. $TiO_2$ shows a strong affinity toward carboxylates, salicylates, and phosphonates.[10,20] These chelating ligands allow the stable anchoring of molecular functions to the surface of $TiO_2$. Modifying the $TiO_2$ surface with various organic molecules affects the selectivity of mass sensors by tuning the interactions between sensor surfaces and VOCs.

In this study, we synthesized a novel series of terthiophene monomers **1**, **2**, **3**, and **4** with a carboxylic acid functionality to modify the $TiO_2$ surface (Figure 1). The amphiphilic monomers were synthesized by metal-catalyzed coupling reactions between methyl 4-(3-(2,5-dibromothienyl))benzoate and thiophene derivatives. Basic hydrolysis in tetrahydrofuran (THF) containing an aqueous solution of potassium hydroxide provided corresponding terthiophene monomers with one carboxylic acid (Scheme 1). Two terminate $\alpha$-positions of terthiophene monomers can be connected with each other by the oxidative polymerization and the carboxylic acid acts as an anchoring group to be adsorbed onto the $TiO_2$ surface. Terthiophene monomers **2** and **3**, where hydrocarbon and perfluorocarbon side chains are directly attached to terthiophene, were synthesized to alter the VOC sensitivity of the sensing layer.

Nanocrystalline $TiO_2$ films were deposited onto the surface of QCMs by spin-coating of $TiO_2$ paste. Low-temperature preparation of porous $TiO_2$ films is necessary to avoid damage to the sensor platforms during the sintering process. We selected an aqueous dispersion of $TiO_2$ particles of roughly 15 nm in diameter to fabricate flexible dye-sensitized solar cells using plastic substrates. Drying $TiO_2$ paste at 120 °C resulted in the formation of robust porous films onto the QCMs without any damage to the sensor platforms. The films were then immersed in a THF solution of terthiophene monomer **1** to give the terthiophene-modified $TiO_2$ films. The adsorption amount of **1** can be monitored by frequency changes in the QCMs. As the immersion period was increased, the frequency decreased and finally saturated after 12 h (see the Supporting Information, Figure S1). The average saturated frequency decrease was 1550 Hz after the adsorption of **1** on $TiO_2$ porous film. The Sauerbrey equation can be used to convert the observed frequency decrease to the adsorption amount of **1** onto the $TiO_2$ porous films.[21] The amount was found to be 1.4 μg on 20 μg $TiO_2$ porous film. The saturated density of **1** on the $TiO_2$ porous film was determined to be $1.6 \times 10^{-10}$ mol $cm^{-2}$, which is close to the reported saturated densities for dyes on the $TiO_2$ porous films in dye-sensitized solar cells.[22] From the molecular dimensions of **1** estimated by computer-generated molecular modeling (Spartan'08), it was estimated that 74% of $TiO_2$ surface area was covered with adsorbed **1**. This ratio suggests that a densely packed monolayer was formed on the $TiO_2$.

The adsorption mode of **1** onto the $TiO_2$ surface was characterized by FT-IR and X-ray photoelectron spectroscopy (XPS). The FT-IR spectrum of **1** reveals the characteristic band of C = O stretch of the carboxylic acid groups at 1680 $cm^{-1}$ (see

the Supporting Information, Figure S2).[22] After the adsorption of **1** onto the $TiO_2$ surface, this band disappeared and the intensities for the symmetric carboxylate band at 1410 $cm^{-1}$ and the asymmetric carboxylate band at around 1620 $cm^{-1}$ increased. The O 1s photoelectron spectrum of the **1**-adsorbed $TiO_2$ film decomposed into three peaks at 530.0, 532.5, and 534.0 eV (see the Supporting Information, Figure S3). Two peaks at 532.5 and 530.0 eV originate from the oxygen atom from the $TiO_2$, and the other peak at 534.0 eV can be attributed to a oxygen atom from the carboxylate group of the adsorbed **1**.[23] These spectral changes indicate the bidentate binding of the deprotonated carboxylate group in **1** to the $TiO_2$ during the adsorption of **1** onto the $TiO_2$ surface. The **1**-adsorbed $TiO_2$ film exhibited two peaks at 165.0 and 166.5 eV in the S 2p photoelectron spectrum, although no peaks were observed in the $TiO_2$ porous film. The adsorption of thiophene derivatives onto metal surfaces has been widely investigated.[24] In general, the S 2p spectra are composed of $2p_{2/3}$ and $2p_{1/3}$ peaks with an intensity ratio of 2:1 and the peaks shift to lower binding energy as a result of binding to the metal surface.[25] The observed two peaks can be assigned to unbound sulfur, indicating that the phenyl spacer between the terthiophene segment and the carboxylic acid in **1** prevents the sulfur atoms from directly interacting with the $TiO_2$ surface.

Electropolymerization of thiophene and oligothiophene monomers to conjugated polymers has been well investigated.[26] Terminal $\alpha$-positions of the terthiophenes are made available for electropolymerization to produce polythiophene and the polymerization of adsorbed terthiophenes results in the covering of the $TiO_2$ surface with the polythiophene layer. Terthiophene segments in the synthesized monomers have a lower oxidation potential necessary for electropolymerization relative to thiophene.[27] Electropolymerization of **1** onto the $TiO_2$ surface was carried out by cyclic voltammetry (CV) using **1**-adsorbed $TiO_2$ films onto the gold electrode of QCM as a working electrode, platinum as a counter electrode, and Ag/AgCl as a reference electrode in a three-electrode cell. The QCM frequency of the **1**-adsorbed $TiO_2$ film after immersion in acetonitrile containing 0.1 M tetrabutylammonium hexafluorophosphate ($TBAPF_6$) and washing it in THF was almost same as that before these treatments, revealing high stability in the adsorption of **1** onto the $TiO_2$ surface. **Figure 2**a shows multiple voltammograms of **1** adsorbed onto the $TiO_2$ film during repeated potential cycling between –0.5 and 1.6 V versus Ag/AgCl. The cyclic voltammograms revealed an irreversible oxidation at 1.1 V versus Ag/AgCl at the first scan, indicating the production of radical cations by the oxidation of the terthiophene monomer. The observed oxidation potential matches the value reported for linear terthiophenes.[28] The CV traces indicate that the oxidation peak shifted slightly to a higher potential and a new peak around 0.2 V versus Ag/AgCl is appeared. The electrochemical response corresponds to the doping/undoping process of the electropolymerized polythiophene layer. The CV traces became constant after the third scan. The porous structure on the QCM was maintained after the electropolymerization of **1** as observed in a field-emission scanning electron microscopy (FE-SEM) image (Figure 2b).

The electropolymerization process was monitored by absorption spectroscopy. The 2-μm-thick $TiO_2$ films were deposited

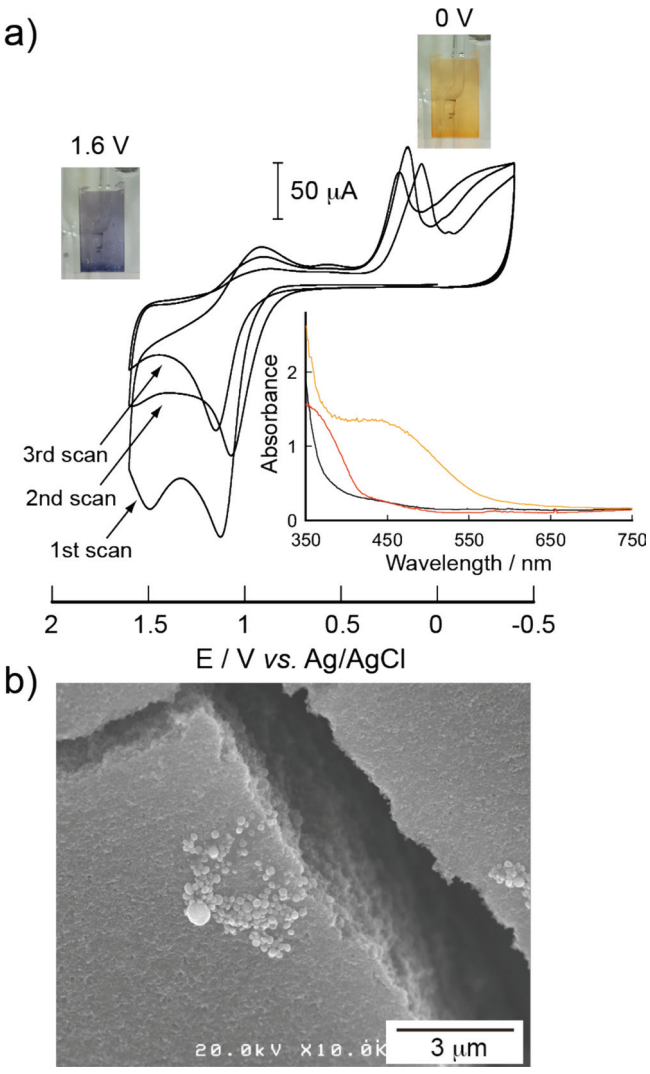


**Figure 2.** a) Cyclic voltammogram of **1** -adsorbed $TiO_2$ porous film on QCM in acetonitrile containing 0.1 M $TBAPF_6$ at room temperature. The polymerization was performed by sweeping from –0.4 to 1.6 V versus a Ag/AgCl reference electrode at 50 mV $s^{-1}$ scan rate, and the electrochromic color change of electropolymerized **1** on a $TiO_2$ porous film deposited onto the ATO transparent electrode at 0 and 1.6 V versus Ag/AgCl is shown. The inset shows absorption spectra of a $TiO_2$ porous film (black line), **1** -adsorbed $TiO_2$ porous film before (red line) and after the electropolymerization (orange line) on ATO electrodes. b) FE-SEM images of $TiO_2$ porous films covered with electropolymerized layer of **1**.

onto transparent antimony-tin oxide (ATO) covered glass and **1** was adsorbed onto the $TiO_2$ surface in the same manner as in $TiO_2$-coated QCMs. The inset of Figure 2a shows the absorption spectra of $TiO_2$-coated ATO substrates before and after the electropolymerization of **1**. The spectrum of **1**-adsorbed $TiO_2$ film has an absorption band around 350 nm, attributed to $\pi$–$\pi^*$ transition of the terthiophene segment. After the electropolymerization of **1**-adsorbed $TiO_2$ film in acetonitrile, containing 0.1 M $TBAPF_6$, the film displays a broad absorption band in the visible region around 450 nm.[27,28] The appearance of this new broad band indicates an extended $\pi$-electronic conjugation along the polythiophene backbones caused by the polymerization of **1**

at the $TiO_2$ surface. Upon oxidation of the electropolymerized film at 1.6 V versus Ag/AgCl, the color of the film changes from orange to blue (Figure 2a).[20] The intensity of the absorption at 450 nm decreases while a new broad band in the near IR region (600–1600 nm) increases in intensity.[24] This spectral change toward the near IR can be assigned to the formation of a stable radical cation or polaronic and bipolaronic species. The electrochromoic switching of this film can be performed over multiple cycles, suggesting a highly reversible redox process for the electropolymerized polythiophene layer onto the $TiO_2$ surface.

When the **1**-adsorbed $TiO_2$ film on the ATO substrate was immersed into an alkaline solution containing THF, the adsorbed **1** completely dissolved into the solution and the absorption band around 350 nm disappeared (see the Supporting Information, Figure S4).[22] On the other hand, the electropolymerized film remained unaltered after the immersion. The frequency change in QCMs coated with electropolymerized film showed only a 5% decrease in weight against the initial adsorption amount of **1** adsorbed onto the $TiO_2$ surface after the immersion in the alkaline solution and careful washing in THF. This shows that the terthiophene monomers adsorbed onto the $TiO_2$ surface can be polymerized by the electrochemical oxidation, and the resulting polythiophene layer is strongly fixed to the $TiO_2$ surface by multiple anchoring through the bidentate coordination of the deprotonated carboxylate group to the $TiO_2$.

We also synthesized the terthiophene monomer **4**, in which the carboxylic acid was directly attached to the terthiophene segment. This monomer **4** also adsorbed onto the $TiO_2$ surface and the saturated density of **4** on the $TiO_2$ porous film ($2.1 \times 10^{-10}$ mol cm$^{-2}$) was slightly higher than that of **1**, revealing the dense packing of **4** onto the $TiO_2$ surface. However, no changes in color and absorption shift of films were observed after the repeated potential cycling, and the oxidized **4** completely dissolved into the alkaline solution. These results indicate that the adsorbed **4**, lacking a phenyl spacer, was not polymerized on the $TiO_2$ surface. This suggests that an optimal conformation freedom is required to allow the electropolymerization of terthiophene monomers adsorbed onto the $TiO_2$ surface. Electropolymerization was successfully achieved when monomers **2** and **3** were adsorbed onto the $TiO_2$ surface. The introduction of hydrocarbon and perfluorocarbon side chains into the terthiophene segment did not affect the electropolymerization process. The $TiO_2$ porous films covered with three different polythiophene layers were obtained through the adsorption of terthiophene monomers onto the $TiO_2$ surface and their subsequent electropolymerization.

The VOC-sensing properties of polythiophene-modified $TiO_2$ porous films on QCMs were investigated by measuring the frequency changes when the film was exposed to various VOC vapors. The measurements consist of an exposure phase and a regeneration phase. During the exposure phase, the films on the QCMs act as sensing layers for target VOC molecules and the interaction of VOC molecules with the sensing layer causes the frequency to decrease. After reaching a constant frequency, the captured VOC molecules are released by supplying pure carrier gas to them. During the regeneration process, the frequency of the sensors rises due to the mass decreasing in the sensing

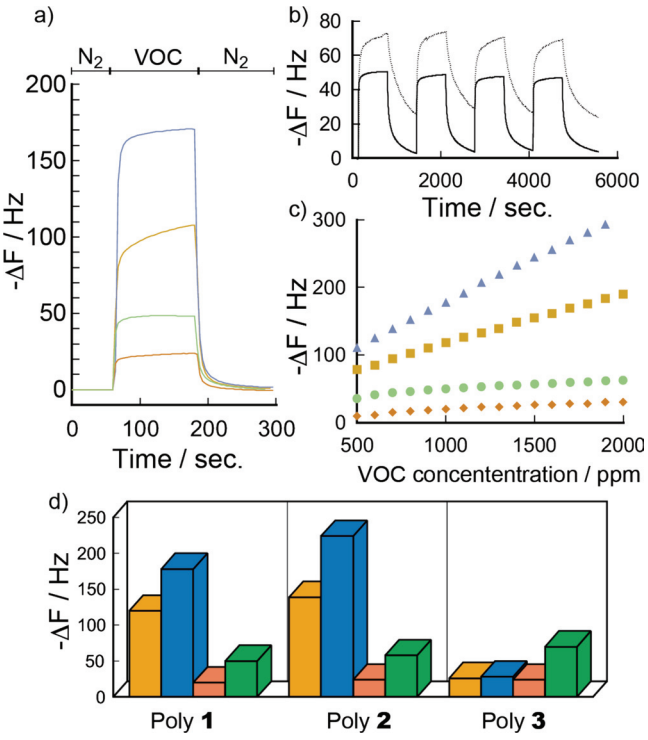


**Figure 3.** a) Frequency changes of QCM sensors deposited with poly **1**/$TiO_2$ on exposure to 1000 ppm VOC vapors (toluene (orange line), n-octane (blue line), ethanol (green line), and acetone (red line)) measured at 20 °C. b) Responses of the QCM sensor with $TiO_2$ (dotted line) and poly **1**/$TiO_2$ (solid line) to repeated dosing with 1000 ppm ethanol vapor. c) Response isotherms of QCM sensors with poly **1**/$TiO_2$ upon exposure to various concentrated VOC vapors. The symbols represent the experimental data for toluene (orange), *n* -octane (blue), ethanol (green), and acetone (red). d) Sensor responses of QCM sensors with poly **1**/$TiO_2$, poly **2**/$TiO_2$, and poly **3**/$TiO_2$ upon exposure to 1000 ppm VOC vapors (toluene (orange), *n* -octane (blue), ethanol (green), and acetone (red)).

layer. The QCM sensors coated with the modified $TiO_2$ films in a temperature-controlled measurement cell at 20 °C were exposed to different VOCs at various concentrations. Toluene, *n*-octane, acetone, and ethanol were chosen as common representatives of different classes of solvents. The sensor responses ($\Delta F$) were obtained from the frequency differences between the corresponding QCM frequencies at the beginning and the end of the exposure phase. **Figure 3**a shows time courses of $\Delta F$ of the QCM sensor deposited with $TiO_2$ porous film covered with polymerized **1** (poly **1**/$TiO_2$) responding to exposure to VOC gases. The QCM sensor coated with only **1** film ($1.0 \pm 0.3$ µm film thickness) exhibited only $-\Delta F = 2$ Hz under exposure to 1000 ppm toluene vapor. In contrast, the sensors with poly **1**/$TiO_2$ responded rapidly and reached $-\Delta F = 110$ Hz within 60 sec. The large and rapid responses can be attributed to the porous structure composed of $TiO_2$ particles owing to their high surface area, as well as the smooth diffusion of gaseous analytes into the porous films.

Figure 3b shows repeated sensor responses of QCM sensors coated with only $TiO_2$ and poly **1**/$TiO_2$ films under exposure to 1000 ppm ethanol vapor. The frequency of the QCM with poly **1**/$TiO_2$ decreased rapidly under the exposure and reached 90%

of the total signal within 30 sec. When the ethanol vapor was switched to pure nitrogen gas, the frequency quickly increased and finally reached the original value within 10 min. These results indicate fast sorption and desorption processes of ethanol vapor at the surface of porous $TiO_2$ covered with a polythiophene layer. However, the sensor coated with only $TiO_2$ porous film exhibited slower sorption and desorption processes and the frequency did not return to the original value after 20 min. The observed slow processes may suggest the contribution of the irreversible sorption of ethanol vapor with Ti–OH sites at the $TiO_2$ surface.

Figure 3c shows the saturated $\Delta F$ values of poly **1**/$TiO_2$-coated sensors in sensing VOCs with various concentrations of 500–2000 ppm. The QCM isotherm to toluene shows two distinct regions including Langmuir-type sorption at lower concentration and Henry-type sorption at higher concentration. This sorption behavior was also observed in the QCM response of gold nanoparticle–polyphenylene dendrimer composite films.[29] Sorption amounts of polar ethanol and acetone were saturated above 1000 ppm, which followed the Langmuir sorption model based on the presence of selective binding sites. Moreover, $\Delta F$ increased linearly as the concentration of nonpolar *n*-octane was increased. This indicates that the properties of VOC gases, such as polarities and boiling points, affect the sorption isotherms. The signal-to-noise ratios or limits of detectability (LOD) of poly **1**/$TiO_2$-coated sensors were measured according to the reported method.[30] We determined a concentration change leading to a signal meeting the signal-to-noise-ratio conventions of the IUPAC (S/N: 3/1). A concentration increase of 10.0 ppm for toluene vapor causes a frequency shift of a 0.7 Hz of poly **1**/$TiO_2$-coated QCM sensor, and the noise level is about 0.2 Hz. The LOD values of poly **1**/$TiO_2$-coated sensors for toluene and *n*-octane were found to be 10 and 6 ppm, respectively.

The response patterns of poly **1**, **2**, and **3**/$TiO_2$-coated sensors, which have different side chains, are shown in Figure 3d. $TiO_2$ porous films covered with three different polythiophenes exhibited different response patterns, suggesting differences in the affinity of the polymers toward VOC vapors. The response sequences of poly **1**, **2**, and **3**/$TiO_2$-coated sensors were *n*-octane > toluene > ethanol > acetone, *n*-octane >> toluene > ethanol > acetone, and ethanol > *n*-octane > toluene = acetone, indicating the selectivity of polymer layers. Poly **2**, with alkyl chains, produced a large response to hydrocarbons, suggesting that *n*-octane interacts with alkyl chains in polythiophene layers through van der Waals force. Poly **3**, with perfluorocarbon chains, showed small responses to acetone, *n*-octane, and toluene and exhibited a large response to ethanol. This shows that introducing side chains into the polythiophene backbone enables the selectivity to be tuned for VOC sensing.

Conductometric sensors rely on the interaction of reducing and oxidizing analyte gases at the surface of semiconductive $TiO_2$ film to cause changes in electrical conduction through the film. Benkstein and Semancik reported the conductometric sensing properties of porous $TiO_2$ films onto microhotplate sensor arrays and showed that the films respond quickly to expose the VOC gases at high operating temperatures around 400 °C.[31] The conductometric sensing property for polythiophene modified $TiO_2$ porous films was investigated by using interdigitated microelectrodes at room temperature. The microelectrodes comprise a series of 36 pairs of interdigitate electrode fingers (1.6 mm in length and 12 μm in width) that are separated by 5 μm. While both $TiO_2$ and poly **1**/$TiO_2$ film displayed small electric current under dark conditions, current–voltage measurements of films showed Ohmic behavior within a range of 0–5 V under the irradiation of 365 nm UV light (see the Supporting Information, Figure S5). The improved conductivity under UV light irradiation is thought to be a generation of extra carriers within $TiO_2$ films by photoexcitation of anatase $TiO_2$.[32] The sensor with poly **1**/$TiO_2$ responded with an increase in resistance upon expose 1000 ppm VOC gases in the dry nitrogen carrier gas under the irradiation of UV light (see the Supporting Information, Figure S5). The resistance responses were significantly slower than those of weight changes monitored by the QCM sensors and the sensitivity to the test vapors decreased in the order toluene > ethanol > acetone > *n*-octane. Thus, the $TiO_2$ films covered with polythiophene layers work as chemically sensitive interfaces to provide two different output signals for the detection of VOCs.

We demonstrated VOC sensing by using microfabricated sensor chips that included four cantilevers. When the cantilevers are coated with the $TiO_2$ porous films covered with different polythiophene layers, the collection of frequency and resistance changes from the microcantilever sensor array provides distinct patterns that allow classification and identification of VOCs (**Figure 4**a). The use of a microdipensing method using a glass microcapillary made it feasible to deposit the $TiO_2$ porous films (about 100 nm film thickness) onto a selected cantilever in an array, treat the cantilever with **1** solution and ferric chloride, and wash it with methanol. Figure 4b shows the responses of a poly **1**/$TiO_2$-coated microcantilever sensor to 1000 ppm VOC vapors.[33] The resonant frequency changed according to the sorption and desorption processes of VOC vapors at the surface of porous $TiO_2$ covered with a polythiophene layer. The resistance changes in the film were simultaneously monitored. The microcantilever sensor coated with poly **1**/$TiO_2$ films produced response isotherms for the frequency and resistance changes that are qualitatively similar to those of QCM sensors and microelectrodes. Moreover, the $TiO_2$ films covered with different polythiophene layers provided different frequency responses for four VOCs (Figure 4c). The responses from the microcantilever sensor array showed a variety of distinct patterns for the detection and discrimination of VOCs.

## 3. Conclusion

To summarize, we have demonstrated that a microcantilever sensor array comprising $TiO_2$ porous films with a large surface area and covered with polythiophene layers can detect VOCs through analyses of frequency and resistance changes in their sensing layer. The large surface area and porosity of the films enhanced their sensitivity to VOC gases due to the internal surface area accessible in them. Covering the $TiO_2$ surface with polythiophene layers improved the repeatability and responsibility for the VOC sensing. Introducing side chains into the polythiophene backbone provided different selectivities for VOCs due to the combination of weak intermolecular interactions between the side chains and VOC gas. This tunability is

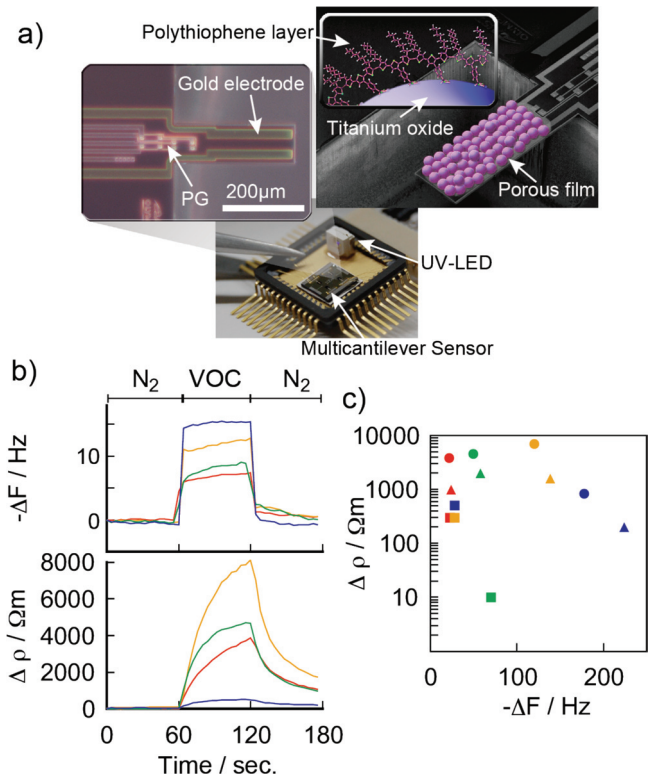


**Figure 4.** a) Optical images of multicantilever sensor mounted on quad flat ceramic package. b) Frequency and resistance responses of poly **1**/$TiO_2$ film on the microcantilever resonator upon exposure to 1000 ppm VOC vapors (toluene (orange), *n*-octane (blue), ethanol (green), and acetone (red)). c) Response pattern obtained from frequency and resistance changes of poly **1**/$TiO_2$ (●), poly **2**/$TiO_2$ (▲), and poly **3**/$TiO_2$ (■) films upon exposure to 1000 ppm VOC vapors (toluene (orange), *n* -octane (blue), ethanol (green), and acetone (red)). The resistance changes were determined at 60 sec.

an important advantage of organic polymers that aids the preparation of a variety of sensing layers for the detection of target VOCs. Previously, we reported the development of a compact chemical sensor system employing a polymer-coated microcantilever sensor array and a thermal preconcentrator. This sensor system succeeded the VOC detection in a sub-ppb concentration range by using ambient carrier gas containing water vapor.[34,35] The experimental results in this study support the claim of the creation of highly sensitive and selective recognition layers for VOC detection. Work is underway in our laboratory to fabricate compact electronic-nose systems to realize on-site and real-time analyses of odors surrounding us under ambient conditions. Research in this area has the potential of eventually enabling the development of electronic nose systems that can continuously monitor odors from our body, which will open up new possibilities for the early detection and the ultimate defeat of cancer.[36]

## 4. Experimental Section

*General*: $^1$H NMR spectra were measured on a Bruker AVANCE 400 FT-NMR spectrometer. Matrix-assisted laser desorption/ionization time-of-flight (MALDI-TOF) mass spectrometry data were obtained using a PerSeptive Biosystems Voyager DE-Pro spectrometer with dithranol as a matrix. FT-IR spectra were obtained using a Shimazu FTIR-8400 spectrometer. UV–vis spectra were measured on a Shimazu MultiSpec-1500 spectrophotometer. Field-emission scanning electron microscopy (FE-SEM) images of porous $TiO_2$ films were recorded in a Hitachi S-5000 FE-SEM without any sputter coating.

*Materials*: All chemicals were purchased from commercial suppliers and used without purification. All solvents were distilled before each procedure. The purification of product was carried out by the combination of adsorption column chromatography (silica gel, Wakogel C-200) and recycling preparative HPLC (Japan Analytical Industry, Model LC-908). Analytical thin-layer chromatography was performed on commercial Merck plates coated with silica gel 60 $F_{254}$.

*Syntheses of Amphiphilic Terthiophene Monomers 1, 2, 3, and 4*: Terthiophene monomers with a carboxylic acid were synthesized by the three or five synthetic steps (**Scheme 1**).

*Methyl 4-(3-(2,5-dibromothienyl))benzoate*: *N*-Bromosuccinimide (NBS) (0.86 g, 4.81 mmol) was added to the solution of methyl 4-(3-thienyl)-benzoate (0.42 g, 1.93 mmol) in dry *N*,*N*-dimethylformamide (DMF) (10 mL) at room temperature. The reaction mixture was stirred for 6 h and was poured into water. After extraction with $CH_2Cl_2$, the organic layer was dried over magnesium sulfate and the solvent was evaporated. The residue was purified by column chromatography on silica gel using $CH_2Cl_2$ as eluent to give methyl-4-(3-(2,5-dibromothienyl))benzoate as white solid (0.63 g, yield 75%). $^1$H NMR ($CDCl_3$, 400.13 MHz): $\delta$ (ppm) = 7.96 (2H, d, $J$ = 8.8 Hz, Ar*H*), 7.33 (2H, d, $J$ = 8.0 Hz, Ar*H*), 6.86 (1H, s, thiophene), 3.90 (3H, s, $CH_3$).

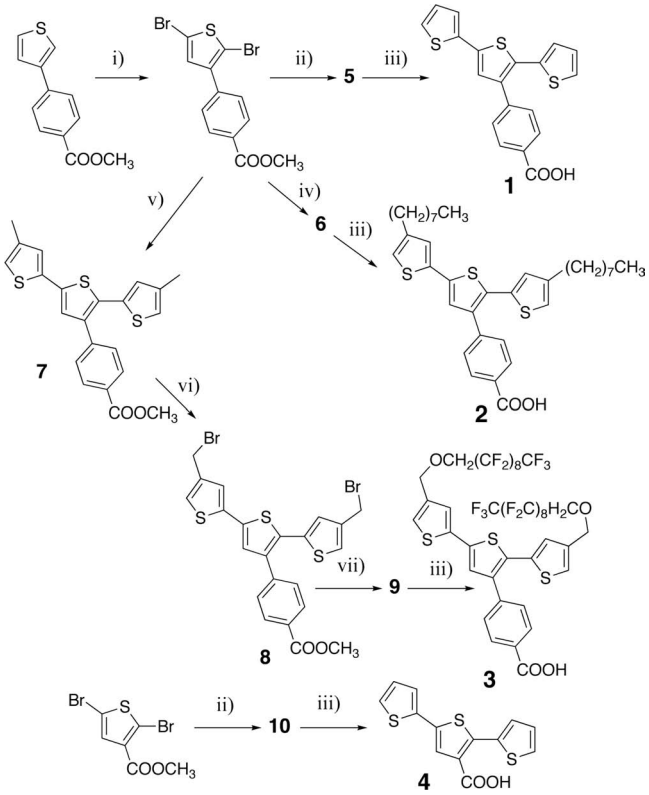


**Scheme 1.** Syntheses of amphiphilic terthiophene monomers **1** – **4**. Reagents and conditions: i) NBS, dry DMF; ii) tributyl(2-thienyl)stannane, $Pd(PPh_3)_4$, DMF; iii) aqueous KOH, THF; iv) 4-octylthiophene-2-boronic acid, $Pd(PPh_3)_4$, toluene, THF, 3.0 M aqueous $Na_2CO_3$; v) 4-methylthiophene-2-boronic acid pinacol ester, $Pd(PPh_3)_4$, toluene, THF, aqueous $Na_2CO_3$; vi) NBS, AIBN, $CCl_4$; vii) 1H,1H-nonadecafluoro-1-decanol, $K_2CO_3$, acetone.

*Synthesis of* **1**: A solution of tributyl(2-thienyl)stannane (1.03 ml, 3.26 mmol), methyl 4-(3-(2,5-dibromothienyl))benzoate (0.49 g, 1.30 mmol), and $Pd(PPh_3)_4$ (0.18 g, 0.155 mmol) in dry DMF (7 mL) was stirred at 100 °C for 48 h under nitrogen. After cooling to room temperature, the reaction mixture was poured into water, extracted with $CH_2Cl_2$ and washed with aqueous 1.0 M KF solution to remove tributyltin chloride. The organic layer was dried over magnesium sulfate and the solvent was evaporated. The residue was purified by column chromatography on silica gel using $CH_2Cl_2$ as eluent to give **5** as a pale yellow solid (0.25 g, yield 51%). FT-IR (ATR); $\nu = 1708$ cm$^{-1}$ (–$COOCH_3$). $^1$H NMR ($CDCl_3$, 400.13 MHz): $\delta$ (ppm) = 7.92 (2H, d, $J$ = 8.0 Hz, Ar*H*), 7.34 (2H, d, $J$ = 8.0 Hz, Ar*H*), 7.24 (2H, d, $J$ = 6.4 Hz, thiophene), 7.06 (2H, m, thiophene), 6.98 (1H, s, thiophene), 6.87 (2H, t, $J$ = 6.0 Hz, thiophene), 3.94 (3H, s, C*H*$_3$). $^{13}$C NMR ($CDCl_3$, 100.61 MHz): $\delta$ (ppm) = 167.1, 144.0, 141.0, 137.7, 130.5, 127.2, 126.4, 125.1, 124.0, 52.2.

To a solution of **5** (0.25 g, 0.654 mmol) in tetrahydrofurane (THF) (7 mL) was added 2 mL of 1.0 M KOH aqueous solution, and the resulting mixture was stirred at 80 °C for 6 h. The reaction mixture was poured into water, extracted with $CH_2Cl_2$ and washed with 0.1 M HCl aqueous solution for neutralization. The organic layer was dried over magnesium sulfate and the solvent was evaporated to give **1** (0.2 g, yield 83%). FT-IR (ATR); $\nu = 1681$ cm$^{-1}$ (–COOH).

*Synthesis of* **2**: 4-Octylthiophene-2-boronic acid (0.69 g, 2.86 mmol) and methyl 4-(3-(2,5-dibromothienyl))benzoate (0.43 g, 1.15 mmol) were dissolved in the mixed solvent of toluene (6 mL), THF (8 mL), and 2.0 M $Na_2CO_3$ aqueous solution (4 mL). After degassing by nitrogen gas, $Pd(PPh_3)_4$ (30 mg, 26.0 μmol) was added to the mixed solution. The reaction mixture was stirred at 70 °C for 48 h under nitrogen atmosphere. After 48 h, the reaction mixture was diluted with diethyl ether (50 mL) and washed with water. The organic layer was dried over magnesium sulfate and concentrated under vacuum. The residue was purified by column chromatography on silica gel using $CH_2Cl_2$ as eluent to give **6** (0.47 g, yield 68%). FT-IR (ATR); $\nu = 1714$ cm$^{-1}$ (-$COOCH_3$). $^1$H NMR ($CDCl_3$, 400.13 MHz): $\delta$ (ppm) = 7.58 (2H, d, $J$ = 8.8 Hz, Ar*H*), 7.23 (2H, d, $J$ = 8.0 Hz, Ar*H*), 7.41 (1H, s, thiophene), 6.90–6.75 (4H, m, thiophene), 3.94 (3H, s, C*H*$_3$), 2.62 (4H, t, $J$ = 7.6 Hz, –C*H*$_2$–), 1.60-1.63 (4H, m, –C*H*$_2$–), 1.28–1.32 (20H, m, –C*H*$_2$–), 0.88 (6H, t, $J$ = 6.8 Hz, –C*H*$_3$). $^{13}$C NMR ($CDCl_3$, 100.61 MHz): $\delta$ (ppm) = 168.1, 144.6, 143.9, 141.3, 139.3, 138.4, 1314, 129.8, 127.3, 125.0, 120.6, 119.8, 48.5, 34.0, 31.9, 30.6, 29.4, 29.3, 22.7. MALDI-TOF-Ms: $m/z$ = 663 ([M+H]$^+$, 100%). Compound **2** was synthesized by the hydrolysis of ester group in **6** by the same procedure of **1**. Yield = 66%. FT-IR (ATR): $\nu = 1682$ cm$^{-1}$ (–COOH). MALDI-TOF-Ms: $m/z$ = 649 ([M+H]$^+$, 100%).

*Synthesis of* **3**: Compound **7** was synthesized from 4-methylthiophene-2-boronic acid pinacol ester (0.67 g, 2.98 mmol) and methyl 4-(3-(2,5-dibromothienyl))benzoate (0.44 g, 1.19 mmol) by the same procedure as **6**. Yield: 55%. FT-IR (ATR); $\nu$ = 1710 cm$^{-1}$ (–$COOCH_3$). $^1$H NMR ($CDCl_3$, 400.13 MHz): $\delta$ (ppm) = 8.02 (2H, d, $J$ = 8.8 Hz, Ar*H*), 7.47 (2H, d, $J$ = 8.4 Hz, Ar*H*), 7.10 (1H, s, thiophene), 7.01 (1H, s, thiophene), 6.84–6.80 (3H, m, thiophene), 3.93 (3H, s, C*H*$_3$), 2.27 (3H, s, –C*H*$_3$), 2.18 (3H, s, –C*H*$_3$). *N*-Bromosuccinimide (NBS) (0.28 g, 1.52 mmol), **7** (0.27 g, 0.66 mmol), and azobisisobutyronitrile (AIBN) (1.0 mg, 5.76 μmol) in 20 mL of $CCl_4$ were refluxed with stirring under nitrogen atmosphere for 6 h. After filtration to remove the reacted succinimide, the solvent was removed to give the brominated compound **8** (0.26 g, 72%) as a pale yellow solid, which was used without further purification. The bromination was checked by $^1$H NMR spectra. $^1$H NMR ($CDCl_3$, 400.13 MHz): $\delta$ (ppm) = 8.05 (2H, d, $J$ = 8.0 Hz, Ar*H*), 7.45 (2H, d, $J$ = 7.2 Hz, Ar*H*), 7.01 (1H, s, thiophene), 6.84–6.80 (4H, m, thiophene), 4.42 (2H, s, –C*H*$_3$), 4.32 (3H, s, –C*H*$_3$), 3.94 (3H, s, C*H*$_3$).

Compound **7** (0.19 g, 0.34 mmol), 1H,1H-nonadecafluoro-1-decanol (0.55 g, 1.10 mmol), and $K_2CO_3$ (4.70 g, 33.6 mmol) in 10 mL of acetone were refluxed overnight. The mixture was filtrated and the solvent was removed. The residue was purified by recrystallization three times from methanol to give **9** (40 mg, 8%). FT-IR (ATR); $\nu = 1722$ cm$^{-1}$ (–$COOCH_3$). $^1$H NMR ($CDCl_3$, 400.13 MHz): $\delta$ (ppm) = 8.05 (2H, d, $J$ = 8.0 Hz, Ar*H*), 7.43 (2H, d, $J$ = 7.6 Hz, Ar*H*), 7.22 (2H, s, thiophene), 7.07 (1H, s, thiophene), 6.90 (2H, s, thiophene), 4.61 (2H, s, –C*H*$_2$–), 4.54 (2H, s, –C*H*$_2$–), 3.95 (4H, m, –C*H*$_2$–), 3.93 (3H, s, C*H*$_3$). MALDI-TOF-Ms: $m/z$ = 1303 ([M+H]$^+$, 100%). Compound **3** was synthesized by the hydrolysis of ester group in **9** by the same procedure of **1**. Yield: 75%. FT-IR (ATR); $\nu$ = 1701 cm$^{-1}$ (-COOH). MALDI-TOF-Ms: $m/z$ = 1289 ([M+H]$^+$, 100%).

*Synthesis of* **4**: Compound **10** was synthesized from tributyl(2-thienyl)-stannane (1.03 ml, 3.26 mmol) and 2,5-dibromo-3-thieophene carboxylic acid methyl ester (0.31 g, 1.03 mmol) by the same procedure of **6**. Yield: 34%. FT-IR (ATR); $\nu = 1714$ cm$^{-1}$ (–$COOCH_3$). $^1$H NMR ($CDCl_3$, 400.13 MHz): $\delta$ (ppm) = 7.48–7.03 (m, 7H, thiophene), 3.94 (3H, s, C*H*$_3$). $^{13}$C NMR ($CDCl_3$, 100.61 MHz): $\delta$ (ppm) = 163.3, 149.6, 141.7, 135.9, 127.9, 127.6, 125.3, 124.4, 51.8. Compound **4** was synthesized by the hydrolysis of ester group in **10** by the same procedure of **1**. Yield: 90%. FT-IR (ATR); $\nu = 1701$ cm$^{-1}$ (–COOH). $^{13}$C NMR ($CDCl_3$, 100.61 MHz): $\delta$ (ppm) = 160.7, 150.5, 135.5, 133.2, 129.8, 127.4, 125.5, 124.7.

*Chemical Sensing of VOCs by modified QCM and Microcanlilever Sensors*: QCM sensors (TamaDevice Co., Ltd., diameter of gold electrode: 5.0 mm) consists of a disk-shaped AT-cut piezoelectronic quartz crystal deposited with gold electrodes on both sides, and are operated at a frequency of 9 MHz. Microcantilever arrays have been fabricated according to the previously reported procedures from single crystal silicone (a dimension of cantilever: 100 μm width, 300 μm length, and 5 μm thickness).[34] The deflection of the cantilevers detected electrically by a set of four-bridged piezoresistive gauges (PGs)) and two gold electrodes with a 30 μm distance were deposited on top surface of the cantilevers. The single sensor chip (5 mm × 5 mm) including four cantilevers was glued on a lead zirconate titanate (PZT) plate of 0.5 μm thick using silver paste to give vibration, and these units were mounted on a 48-pin quad flat ceramic package. UV LED lamp (NitrideSemiconductors Co. Ltd., NS365-7SFF) was also mounted on the same package for the illumination with 365 nm UV light. The PGs, gold electrodes, PZT plate, and UV LED were electrically connected by gold bonding wires (wire diameter is 25 μm) to the package leads. A network analyzer (Agilent Technologies, 4395A) was employed to measure the vibration characteristics of the cantilever sensor, where signal input and output were connected with PZT plate electrodes and bridged output of the PGs, respectively. DC voltages were supplied to the PGs and UV LED from voltage sources. The cantilever was driven at around 420 KHz by the use of feedback oscillation circuit for self-oscillation, which was comprised of signal amplifier, phase controller, band pass filter, and automatic gain controller (see the Supporting Information, Figure S6). This circuit allows us selective oscillation of higher vibration modes of the cantilever by adjusting the band pass filter.

$TiO_2$ porous films were prepared by the deposition of nanocrystalline $TiO_2$ paste (Showa Denko, SP-210) onto the surface of QCM or microcantilever by spin-coating and microdipensing methods, and the following sintering at 120 °C for 20 min. After sintering, the thickness of the $TiO_2$ porous films was measured with a profilometer (Kosaka Laboratory Ltd., ET-4000). The modified sensors were immersed into 0.2 mM terthiophene monomers in THF and left for 12 h at room temperature. After 12 h, the sensors were washed with THF for several times to remove free terthiophenes and dried at 75 °C. Adsorbed terthiophenes were polymerized by the electrochemical oxidation in acetonitrile containing 0.1 M $TBAPF_6$ or the chemical oxidation by $FeCl_3$. The deposition of porous $TiO_2$ films on the gold electrodes, the adsorption of terthiophene monomers, and the sensor responses can be evaluated by determining the frequency changes.

VOC sensitivities of the sensing layers on QCM, microelectrode, and microcantilever sensors were investigated using a temperature-controlled chamber designed for measuring simultaneously frequency change and the response of resistance. (see the Supporting Information, Figure S6). Test vapors of toluene, *n*-octane, ethanol, and acetone were generated by the gas calibration unit using ultrapure nitrogen gas as a carrier gas. Diluted gases are led into the measuring chamber by the computer-driven magnetic valve systems. The frequency and resistance changes of sensors were monitored in response to the incorporation of VOCs. Temperature in the measuring chamber was stabilized by a Peltier thermostat to avoid the temperature-dependent frequency changes and temperature of the chamber was monitored during the experiments. Six

universal frequency counters (Agilent Technology, Model 53131A) are able to determine twelve frequencies at the same time. The resistance changes during the VOC sorption are monitored by a source meter (Keithley Instruments Inc., Model 2602).

## Supporting Information

Supporting Information is available from the Wiley Online Library or from the author.

## Acknowledgements

This work was partially supported by "Regional Innovation Cluster Program of Nagano" from the Ministry of Education, Culture, Sports, Science, and Technology, Japan.

Received: August 19, 2011
Published online: November 25, 2011

[1] L. Buck, R. Axel, *Cell* **1991**, *65*, 175–187.
[2] *Handbook of Machine Olfaction Electronic Nose Technology*: (Eds: T. C. Pearce, S. S. Schiffman, H. T. Nagle, J. W. Gardner), Wiley-VCH, Weiheim **2003**.
[3] F. Röck, N. Barsan, U. Weimar, *Chem. Rev.* **2008**, *108*, 705–725.
[4] K. J. Albert, N. S. Lewis, C. L. Schauer, G. A. Sotzing, S. E. Stitzel, T. P. Vaid, D. R. Walt, *Chem. Rev.* **2000**, *100*, 2595–2626.
[5] N. A. Rakow, K. S. Suslick, *Nature* **2000**, *406*, 710–713.
[6] S. H. Lim, L. Feng, J. W. Kemling, C. J. Musto, K. S. Suslick, *Nat. Chem.* **2009**, *1*, 562–567.
[7] T. Nakamoto, H. Ishida, *Chem. Rev.* **2008**, *108*, 680–704.
[8] S. Joo, R. B. Brown, *Chem. Rev.* **2008**, *108*, 638–651.
[9] D. V. Talapin, J.-S. Lee, M. V. Kovalenko, E. V. Shevchenko, *Chem. Rev.* **2010**, *110*, 389–458.
[10] M. Grätzel, *Nature* **2001**, *414*, 338–344.
[11] M. Josowicz, J. Janata, *Anal. Chem.* **1986**, *58*, 514–517.
[12] J. Janata, M. Josowicz, *Nat. Mater.* **2003**, *2*, 19–24.
[13] B. J. Holliday, T. B. Stanford, T. M. Swager, *Chem. Mater.* **2006**, *18*, 5649–5651.
[14] B. Li, S. Santhanam, L. Schultz, M. Jeffries-EL, M. C. Iovu, G. Sauvé, J. Cooper, R. Zhang, J. C. Revelli, A. G. Kusne, J. L. Snyder, T. Kowalewski, L. E. Weiss, R. D. McCullough, G. K. Fedder, D. N. Lambeth, *Sens. Actuators B* **2007**, *123*, 651–660.
[15] Y. S. Jung, W. Jung, H. L. Tuller, C. A. Ross, *Nano. Lett.* **2008**, *8*, 3776–3780.
[16] M. Xue, Y. Zhang, Y. Yang, T. Cao, *Adv. Mater.* **2008**, *20*, 2145–2150.
[17] B. Esser, T. M. Swager, *Angew. Chem. Int. Ed.* **2010**, *49*, 8872–8875.
[18] A. M. Taurino, S. Capone, A. Boschetti, T. Toccoli, R. Verucchi, A. Pallaro, P. Siciliano, S. Iannotta, *Sens. Actuators B* **2004**, *100*, 177–184.
[19] B. L. Zhu, C. S. Xie, W. Y. Wang, K. J. Hung, J. H. Hu, *Mater. Lett.* **2004**, *58*, 624–629.
[20] D. Cummins, G. Boschloo, M. Ryan, D. Corr, S. N. Rao, D. Fitzmaurice, *J. Phys. Chem. B* **2000**, *104*, 11449–11459.
[21] G. Sauerbrey, *Z. Phys.* **1959**, *155*, 206–222.
[22] H. Imahori, Y. Matsubara, H. Iijima, T. Umeyama, Y. Matano, S. Ito, M. Niemi, N. V. Tkachenko, H. Lemmetyinen, *J. Phys. Chem. C* **2010**, *114*, 10656–10665.
[23] E. M. J. Johansson, M. Hedlund, H. Siegbahn, H. Rensmo, *J. Phys. Chem. B* **2005**, *109*, 22256–22263.
[24] J. Noh, E. Ito, K. Nakajima, J. Kim, H. Lee, M. Hara, *J. Phys. Chem. B* **2002**, *106*, 7139–7141.
[25] F. Buckel, F. Effenberger, C. Yan, A. Gölzhäuser, M. Grunze, *Adv. Mater.* **2000**, *12*, 901–904.
[26] R. D. McCullough, *Adv. Mater.* **1998**, *10*, 93–116.
[27] R. Ponnapati, M. J. Felipe, J. Y. Park, J. Vargas, R. Advincula, *Macromolecules* **2010**, *43*, 10414–10421.
[28] C. D. Grande, M. C. Tria, G. Jiang, R. Ponnapati, R. Advincula, *Macromolecules* **2011**, *44*, 966–975.
[29] N. Krasteva, Y. Fogel, R. E. Bauer, K. Müllen, Y. Joseph, N. Matsuzawa, A. Yasuda, T. Vossmeyer, *Adv. Funct. Mater.* **2007**, *17*, 881–888.
[30] F. L. Dickert, P. Forth, P. Lieberzeit, M. Tortschanoff, *Fresenius J. Anal. Chem.* **1998**, *360*, 759–762.
[31] K. D. Benkstein, S. Semancik, *Sens. Actuators B* **2006**, *113*, 445–453.
[32] N. Kumazawa, M. R. Islam, M. Takeuchi, *J. Electroanal. Chem.* **1999**, *472*, 137–141.
[33] All four cantilevers were coated with $TiO_2$porous films covered with poly **1**.
[34] T. Mihara, T. Ilehara, J. Lu, R. Maeda, T. Fukawa, M. Kimura, Y. Liu, T. Hirai, *AIP Conf. Proc.* **2009**, *1137*, 79–82.
[35] T. Mihara, T. Ikehara, M. Konno, R. Maeda, M. Kimura, T. Fukawa, *Sens. Mater.* **2011**, *27*, 397–417.
[36] G. Peng, U. Tisch, O. Adams, M. Hakim, N. Shehada, Y. Y. Broza, S. Billan, R. Abdah-Bortnyak, A. Kuten, H. Haick, *Nat. Nanotechnol.* **2009**, *4*, 669–673.